



Room-temperature workability of 6063 alloy for fitting clamps of overhead conductor lines



L.R. Zeng^a, Z.M. Song^a, X.M. Wu^b, C.H. Li^b, G.P. Zhang^{a,*}

^a Shenyang National Laboratory for Materials Science, Institute of Metal Research, Chinese Academy of Sciences, Shenyang 110016, China

^b Institute of Electrical Power Research, Electrical Power Limited Company of Liaoning Province, Shenyang 110006, China

ARTICLE INFO

Article history:

Received 21 June 2014

Accepted 7 September 2014

Available online 16 September 2014

Keywords:

Aluminum alloy

Compressive workability

Schmid factor

Misorientation

ABSTRACT

Compression workability of the 6063 aluminum alloy for fitting clamps to fasten and connect the aluminum alloy conductor lines was investigated under different height reductions and strain rates at room temperature. The deformation map for compression workability is obtained, which provides the critical deformation conditions related to deformation reduction and strain rate below which the 6063 alloy can be safely processed without cracking damage. Cracking damage behavior was investigated by electron backscattering diffraction technique, revealing that the compression-induced cracking of the 6063 alloy tends to occur at the grain boundaries with grain boundary misorientation angles more than 47°.

© 2014 Elsevier Ltd. All rights reserved.

1. Introduction

The 6063 alloy, a kind of Al–Mg–Si alloy, is a good candidate not only for the medium-strength overhead conductor lines [1,2], but also for fitting clamps to fasten and connect the aluminum alloy conductor lines [3,4]. To have the conductor lines connected, the fitting clamp is usually mechanically compressed to a certain amount of plastic deformation at a proper strain rate with a hydraulic compression machine. Such that, two bundles of the conductor lines threading the clamp can be fastened. However, during the cold working process, the deformation-induced damage, such as microcracks or voids, is frequently introduced into the fitting clamp due to the large deformation and the high strain rate [5,6]. A number of investigations on the 6063 alloy mainly focus on strength [7], deformation behavior at room temperature [8,9] and high temperature [10,11]. Gunduz and Kacar [7] investigated strengthening of 6063 aluminum alloy by strain aging, and found that the variations in aging time have improved the mechanical properties of the 6063 Al-alloy, whereas the ductility has decreased. Balogun et al. [8] found that forging and rolling at room temperature (RT) could increase dislocation motion while still improving the ultimate tensile strength and hardness, they also found that the forging process caused the gaseous pores to move by spreading them along the forging direction, thus reducing the rate of crack growth and damage. Ko et al. [9] investigated the microstructure and mechanical properties of 6063 Al alloy

fabricated by shear-drawing technique, and revealed the optimum condition for sound deformation of the alloy subjected to a combination of shear and drawing strains within a predetermined die. Panigrahi et al. [12,13] studied the effect of plastic deformation conditions (rolling temperature, rolling strain) on microstructural characteristics of the 6063 alloy. They found that cryogenic temperature deformation can suppress the dynamic recovery and builds up a higher dislocation density in the samples than the RT deformation. For the workability of the 6063 alloy at room temperature, the relationship between cracking damage and cold-working parameters (the strain rate and deformation reduction) has not been well established and understood yet.

In this paper, effects of different deformation reductions and strain rates on deformation and cracking behaviors of the 6063 alloy are investigated at RT. The relations among cracking, misorientation of grain boundary (GB) and Schmid factor are examined. Furthermore, the compression workability of the alloy at RT is evaluated for the potential applications.

2. Materials and experimental procedures

As a fitting clamp to fasten and connect the aluminum alloy conductor lines, the extruded 6063 alloy subjected to solid solution treatment only was selected in the present study. The nominal chemical compositions of the alloy are shown in Table 1. To conduct mechanical testing, compressive specimens with dimensions of $5 \times 5 \times 10 \text{ mm}^3$ were fabricated by a spark cutting machine, and then subjected to mechanical polishing. Finally, the specimens were electropolished carefully.

* Corresponding author. Tel./fax: +86 24 23971938.

E-mail address: gpzhang@imr.ac.cn (G.P. Zhang).

Table 1
Chemical compositions (wt%) of 6063 aluminum alloy.

Mg	Si	Fe	Cu	Ti	Zn	Al
0.45–0.9	0.2–0.6	<0.3	<0.1	<0.1	<0.1	Bal.

To reduce the friction between the top and the bottom surfaces of the compression specimen and loading heads, the top and bottom surfaces of the specimen were coated by Teflon film with a thickness of 0.05 mm prior to the compression tests. All the compression tests were performed using a commercial mechanical testing machine (Instron® 8801). The specimens were subjected to different reductions of height ranging from 25% to 70% and strain rates from 1×10^{-5} to $1 \times 10^{-1} \text{ s}^{-1}$. The deformation morphologies at the specimen surfaces were characterized by scanning electron microscopy (SEM, Leo Supra 35) after compressive tests. The electron back scattering diffraction (EBSD) technique is used to identify the GB misorientation angles and Schmid factors of the deformed grains. Microstructures before and after deformation were examined by transmission electron microscopy (FEI Tecnai F20).

3. Results

3.1. Microstructure

Fig. 1(a) presents an EBSD inverse pole figure (IPF) of grain distribution of the as-received 6063 alloy subjected to solid solution treatment. One can see that the equiaxed grains have random orientations and their sizes are homogeneous. The mean grain size presented in Fig. 1(b) is 75.2 μm . The IPF in Fig. 1(a) also indicates that the alloy does not have apparent texture.

3.2. Compressive stress–strain response and deformation behavior

Fig. 2 presents typical engineering compressive stress–strain curves of the alloy compressed to 70% reduction of height, showing

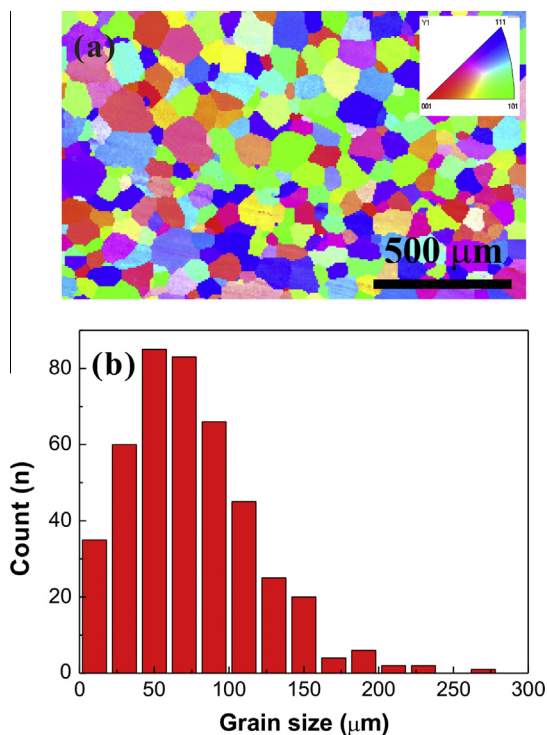


Fig. 1. Microstructure of 6063 aluminum alloy: (a) EBSD analysis; (b) statistic distribution of grain size.

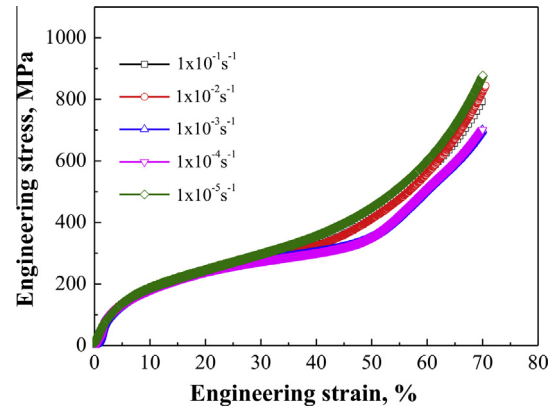


Fig. 2. Engineering stress–strain curves of 6063 alloy deformed compressively by 70% height reduction at different strain rates.

that there is no evident difference in yield strength and compressive stress–strain response at different strain rates ranging from 1×10^{-5} to $1 \times 10^{-1} \text{ s}^{-1}$. Compressive yield strength is estimated to be 75 MPa. The yield stress is evidently lower than that of the alloy after aging treatment [14,15].

Fig. 3 shows SEM micrographs for deformation and cracking morphologies at the specimen surfaces, where some cracking has formed at the certain strain rates and compressive reductions. Comparing deformation behavior of the specimens subjected to the same 25% reduction of height and different strain rates in Fig. 3(a) and (b), one can find that extensive slip bands occurred inside some grains, and GBs became visible under compressive loading due to severe strain incompatibility among grains. Thus, the cracks appear along the GBs, as shown in Fig. 3(c) for the close observation of Fig. 3(b). The number of cracks increases with increasing the strain rate and the compressive reduction. Fig. 3(d) and (e) show that plastic deformation behavior becomes more nonuniform with increasing the strain rate from $1 \times 10^{-4} \text{ s}^{-1}$ to $1 \times 10^{-1} \text{ s}^{-1}$ under the same 45% reduction of height. A close observation (Fig. 3(e)) also indicates cracking along the GB (Fig. 3(f)). In Fig. 3(g)–(i), it is found that the higher strain rate leads to the formation of many small cracks, the number of cracks increases and the length of the cracks decreases with increasing the strain rate. In general, the high strain rate would cause more severe strain incompatibility among the grains, resulting in the occurrence of cracking even under smaller deformation reductions. In contrast, the alloy can sustain relatively large extent of uniform plastic deformation at the lower strain rates.

3.3. Compression workability of the alloy

The possibility of the appearance of microcracks in the alloy subjected to different reductions of height and strain rates is examined through SEM observations of deformation morphologies of specimens. Here, in order to get full information on cracking possibility not only at the surfaces of the specimens but also the interiors of the specimens, the deformed specimens were cut into some pieces so that the sections of the specimens could be carefully checked by the SEM. Fig. 4 shows the statistic formation of internal cracks in the compressively-deformed alloy as functions of reduction of height and strain rate. The hollow circles refer to the occurrence of cracking at the certain strain rate and the deformation reduction, while the solid circles indicate the absence of cracking. It is obvious that the shadow region in the left corner in Fig. 4 is the safety zone, where the working parameters (strain rate and deformation reduction) may be selected for compressive deformation and processing of the alloy, while the working

Download English Version:

<https://daneshyari.com/en/article/828797>

Download Persian Version:

<https://daneshyari.com/article/828797>

[Daneshyari.com](https://daneshyari.com)